Experiments on Large Fluctuations and Optimal Control

Igor Khovanov Dmitri Luchinsky **P.V.E. McClintock**

Department of Physics, Lancaster University

Durham, 5 July 2006

Outline

How do large fluctuations occur? What are optimal paths? How do they manifest in reality?

Mark Dykman (1951 –)

- Fluctuations and nonlinearity are of course universal, affecting all macroscopic physical systems.
- Rare large fluctuations are often the most important, for e.g. –
  - Chemical reactions
  - Mutations in DNA sequences
  - Failures of electronic devices, lasers
  - Stochastic resonance
  - Protein transport in Brownian ratchets
- Aim is it investigate large rare fluctuations, and how they happen –
  - Use an experimental approach
  - Measure, understand, predict
  - Control, exploit?
- Although rare, when large fluctuations arise, they occur in an almost deterministic manner.

Physical picture

Consider overdamped Brownian motion of a particle in the force field $\mathbf{K}(\mathbf{x}, t)$, driven by weak white noise of intensity D...

- Mostly, system fluctuates near a stable state S at $\mathrm{x} = \mathrm{x}_S$ (N.B. figure from book uses $A(t)$ as state variable).
- Very occasionally, a large rare fluctuation takes the system to a remote state x_f – from which it may then return.
- But how does the event occur? One idea, from the 1994 textbook by a distinguished authority...

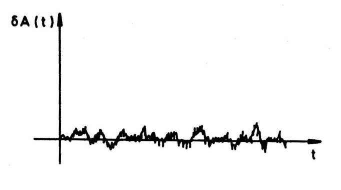

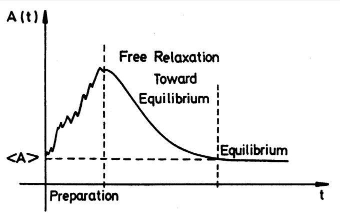

Problem to be solved

- Problem: to describe the form of the trajectories to and from x_f.
- Assumption: the noise is weak, $D \to 0$ (no assumption of adiabaticity). Hamiltonian (or equivalent path-integral approach) –
- Many researchers: Cohen & Lewis (1967), Ventzell & Freidlin (1970), Ludwig (1975), Dykman et al (1979), Graham & Tell (1984), Jauslin (1986), Day (1987), McKane (1989), ...and numerous others, over the last 30 years.
- Start from the Fokker-Planck equation... use the weak noise assumption...
- We consider the simplest one-dimensional example – but the formalism is easily extended.

Finding the "auxiliary system"

Fokker-Plank equation (FPE) for probability density $P(\mathbf{x}, t)$ is

$$\frac{\partial P(\mathbf{x}, t)}{\partial t} = -\nabla \cdot (\mathbf{K}(\mathbf{x}, t) P(\mathbf{x}, t)) + \frac{D}{2} \nabla^2 P(\mathbf{x}, t).$$

Near a stable stationary state S, for $D \to 0$, use WKB (eikonal) approximation

$$P(\mathbf{x}, t) = z(\mathbf{x}, t) \exp\left(-\frac{W(\mathbf{x}, t)}{D}\right).$$

where $z(\mathbf{x}, t)$ is a prefactor, and $W(\mathbf{x}, t)$ is a classical action satisfying the Hamilton-Jacobi equation, which can be solved by integrating the Hamiltonian equations of motion

$$\dot{\mathbf{x}} = \mathbf{p} + \mathbf{K}, \quad \dot{\mathbf{p}} = -\frac{\partial \mathbf{K}}{\partial \mathbf{x}} \mathbf{p},$$

$$H(\mathbf{x}, \mathbf{p}, t) = \mathbf{p}\,\mathbf{K}(\mathbf{x}, t) + \frac{1}{2}\mathbf{p}^2, \quad \mathbf{p} \equiv \nabla W,$$

with Hamiltonian $H(\mathbf{x}, \mathbf{p}, t)$ for appropriate boundary conditions.

Minimum action solutions

In seeking extreme trajectories that minimise the action, we find two different types of solution –

1. Set of Hamiltonian trajectories approaching S
   $\equiv$ stable invarient manifold of S, with $\mathbf{p} = 0$.
2. Set of Hamiltonian trajectories leaving S
   $\equiv$ unstable invarient manifold of S, with $\mathbf{p} \neq 0$.

Note:

- The theory is now deterministic (no D).
- But real physical systems have finite D.
- Extremal paths are not necessarily optimal paths.
- Non-equilibrium systems have singularities.
- Beautiful patterns of extreme trajectories can be drawn.
- Without experiments – not obvious how all this relates to reality!

Example of extreme paths Chinarov et al, *Phys. Rev E* **47**, 2448 (1993).

- Extreme paths for a nearly resonantly driven nonlinear oscillator.
- Caustics are clearly evident.

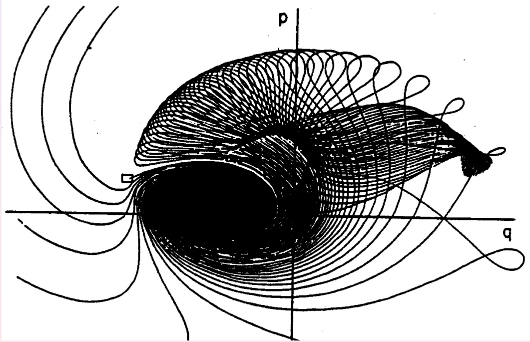

Example of extreme paths

Maier & Stein, *J. Stat. Phys.* **83**, 291 (1996).

Extreme paths for non-potential gradient system

$$K_x(x,y) = x - x^3 - \alpha x y^2$$
$$K_y(x,y) = -\mu(1+x^2)y$$

- Shows outgoing paths from stable point for $\alpha = 1, 4, 5, 10$.
- Note focussing for $\alpha > 4$.

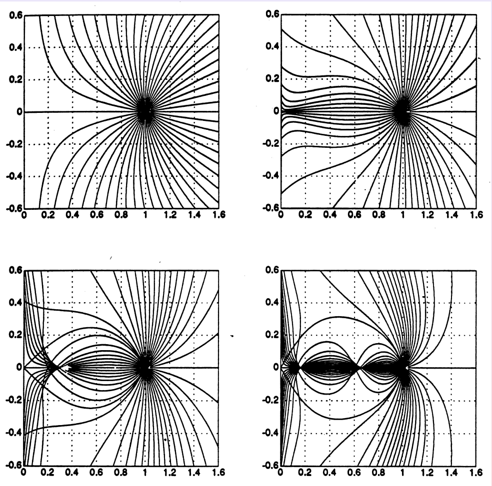

Example of extreme paths

Dykman et al, *Phys. Lett. A* **195**, 53 (1994).

- Periodically driven nonlinear oscillator.
- Again, caustics evident.
- But do real fluctuations ever look like this?
- Where do caustics come from?
- What experiments are possible?

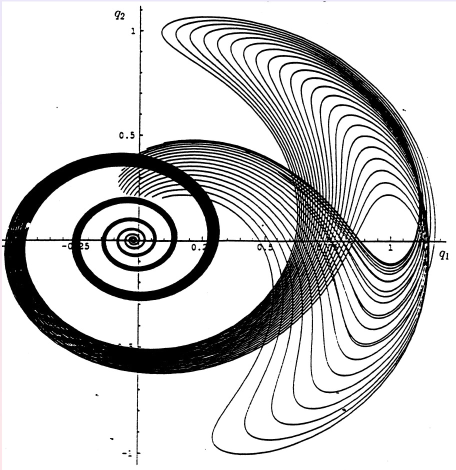

Generation of singularities Dykman et al, *Phys. Lett. A* **195**, 53 (1994).

- Singularities arising from folds in the Lagrangian manifold.
- Caustics arise because paths cannot go beyond fold.
- A pair of caustics emanate from a cusp point.
- Two families of extreme paths: 1 go below cusp; 2 go round above cusp.
- Paths cannot cross switching line, so caustics are not experimental observables.
- But cusp and switching line should be observable.

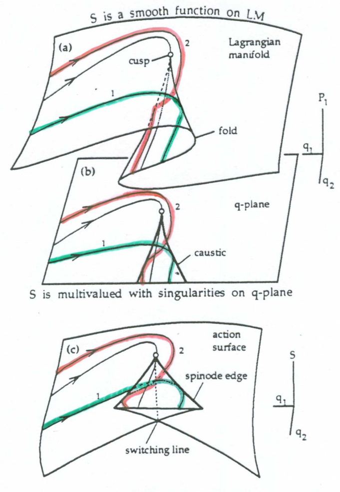

Fig. 2. Generation of singularities.

Experiments on large fluctuations – basic procedure

1. Build model of system –
   - Analogue electronic, or
   - Numerical
2. Apply relevant forces, e.g. noise, periodic force...
3. Measure response –
   - Await arrival at x_f
   - Record arrival path
4. Repeat, ensemble-average, to find prehistory probability distribution $P_h(x, t; x_f, t_f)$.

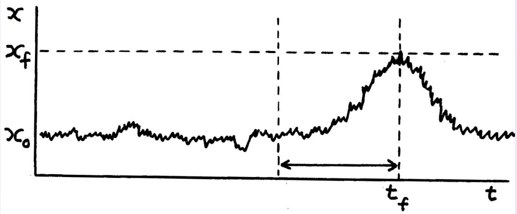

If system departs stable state at $t = -\infty$ and arrives at $x = x_f$ at time $t = t_f$, then $p_h(x, t; x_f, t_f)$ gives probability of being at x at time t.

Very simple example

- Consider overdamped double-well Duffing oscillator driven by zero-mean white noise of intensity D.

$$\begin{aligned}\dot{x} &= -U'(x) + \xi(t),\\ U(x) &= -\frac{1}{2}x^2 + \frac{1}{4}x^4,\\ \langle \xi(t) \rangle &= 0, \quad \langle \xi(t)\xi(t') \rangle = D\delta(t-t').\end{aligned}$$

- Interested in rare fluctuations to a particular final position x_f, far from the equilibrium state.
- Catch segment of path leading to x_f, build the prehistory probability distribution $p_h(x, t; x_f, t_f)$.
- Guess that $p_h(x, t; x_f, t_f)$ is closely connected to the optimal path of the $D \to 0$ theory.

Examples of 2 large fluctuations in circuit model

Differs from earlier sketch –

- Symmetric in time.
- Small fluctuations similar on both fluctuational and relaxational parts of path.

Construct ensemble average to measure prehistory (or posthistory) probability density.

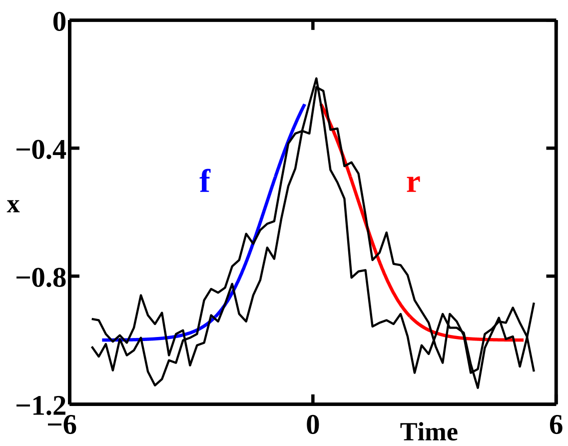

Observation of an optimal path Dykman et al, *PRL* **68**, 2718 (1992).

- Identify ridge (locus of maxima) with the optimal path of the $D \to 0$ Hamiltonian fluctuation theory.
- Note (unpredicted) dispersion just before t_f.

Q: What happens to fluctuation after reaching x_f?

A: It dies!

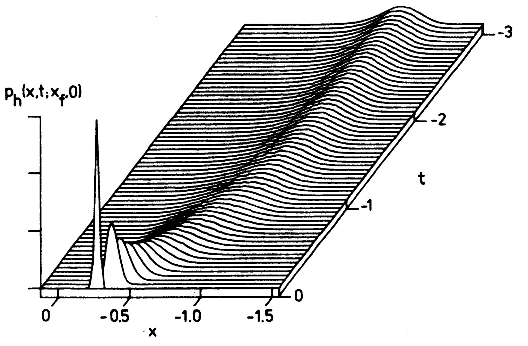

Physical significance of optimal paths

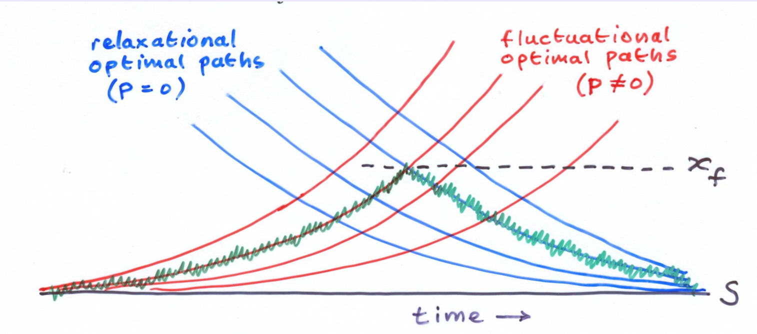

- Determinism only works backwards for fluctuational paths.
- Relaxational paths are deterministic.
- If system is "caught" at x_f then, with overwhelming probability, it switches to relaxational path and returns to S.

Time-reversal symmetry in equilibrium

- Prehistory & posthistory densities.
- Optimal paths plotted in top-plane.
- Blue and red curves are theory.
- Prediction of time-reversal symmetry is verified.

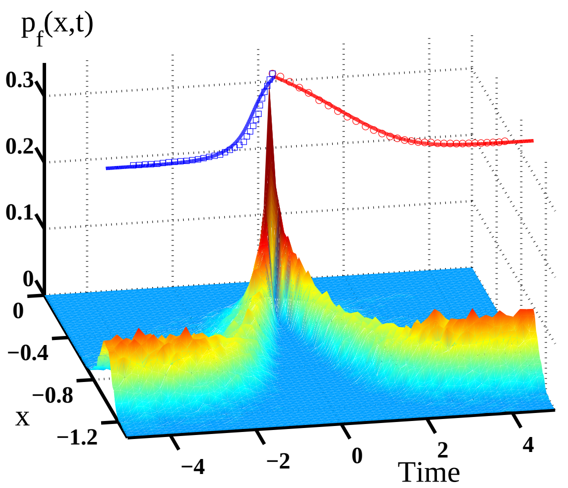

Physical significance of p?

- What is the physical significance of p?
- An "effective momentum" in the theory – is it just a theoretical abstraction?
- No: p represents the force provided by the noise – the rare special noise history producing the rare fluctuation.
- In electronic experiments, can measure p during fluctuation, so can ask –

  Q: Is it true that $p \neq 0$ during fluctuational path, and $p = 0$ during relaxation, as predicted by Hamiltonian theory?

  A: Find out answer from experiment.

(N.B. Unclear how to measure p in a thermal system)

Observation of the optimal force

- Double-well Duffing.
- Densities and (inset) paths.
- Lines are theory.
- Clearly $p \neq 0$ in fluctuational path.
- But $p = 0$ during relaxation.

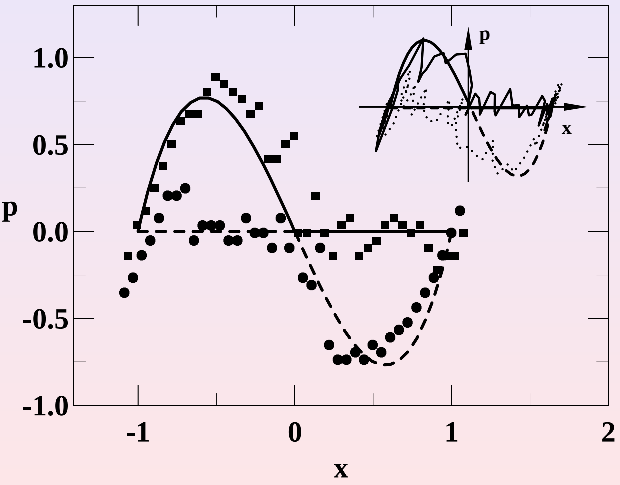

A very simple example

- Consider simplest example – system driven from equilibrium by a periodic force –

$$\dot{x} = -U'(x) + A\cos\omega t + \xi(t),$$
$$U(x) = -\frac{1}{2}x^2 + \frac{1}{4}x^4,$$
$$\langle\xi(t)\rangle = 0, \quad \langle\xi(t)\xi(t')\rangle = D\delta(t-t').$$

  i.e. an overdamped bistable oscillator driven by zero-mean white noise of intensity D and a periodic force of amplitude A, frequency ω.

- Interested in fluctuations to (x_f, t_f), via (x, t), where the time t now determines the phase ϕ of the periodic force.
- The Hamiltonian fluctuation theory is easily worked out...

Hamiltonian theory for double-well Duffing

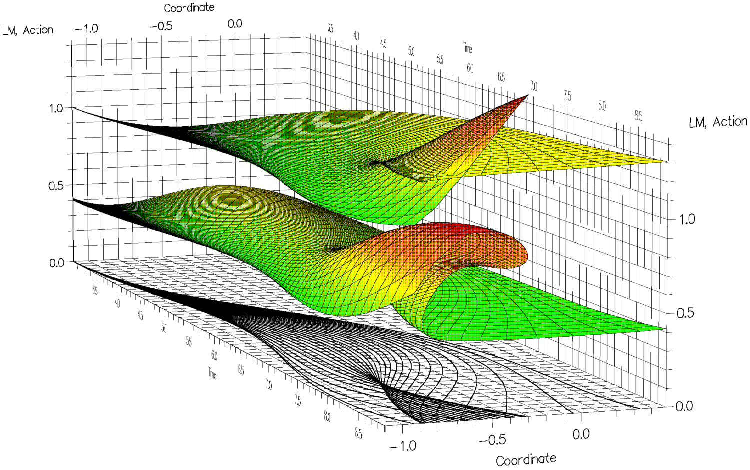

Action surface, Lagrangian manifold, and extreme paths, calculated for periodically-driven double-well Duffing.
D G Luchinsky, *Contemporary Phys.* **45**, 379 (2002).

Measurements on driven double-well Duffing

- (q_f, t_f) on (red) switching line.
- Hence corral of optimal paths.
- Sensitive to small departures from switching line.
- Top-plane shows experiment (green dots) and theory (blue lines).

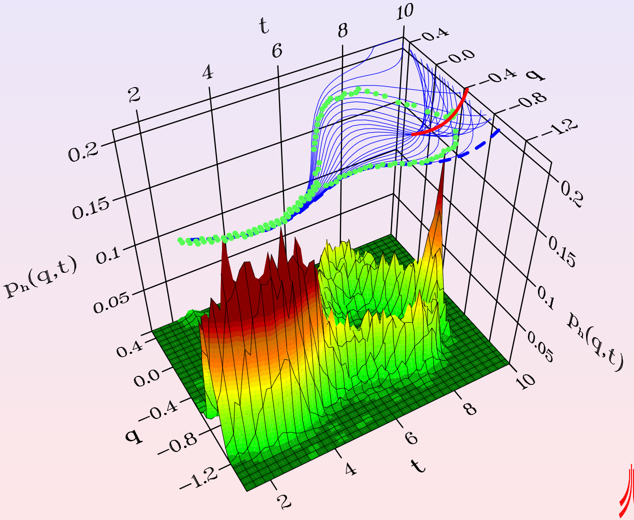

Maier and Stein system

- Consider Maier & Stein's system – an overdamped oscillator driven from equilibrium by a stationary nongradient field –

$$\begin{aligned} \dot{x} &= x - x^3 - \alpha x y^2 + f_x(t) \\ \dot{y} &= -\mu y(1 + x^2) + f_Y(t) \\ \langle f_i(t) \rangle &= 0, \quad \langle f_i(s) f_j(t) \rangle = \epsilon \delta_{ij} \delta(s - t) \end{aligned}$$

- A nongradient system (unless $\alpha = 1$), so dynamics not governed by detailed balance.
- Investigate an electronic model.

Maier & Stein system prehistory densities

- Combination of data from two experiments with $\pm y_f$, same x_f.
- Points on top-plane from ridge of prehistory density.
- Lines on top-plane from $\epsilon \to 0$ theory.

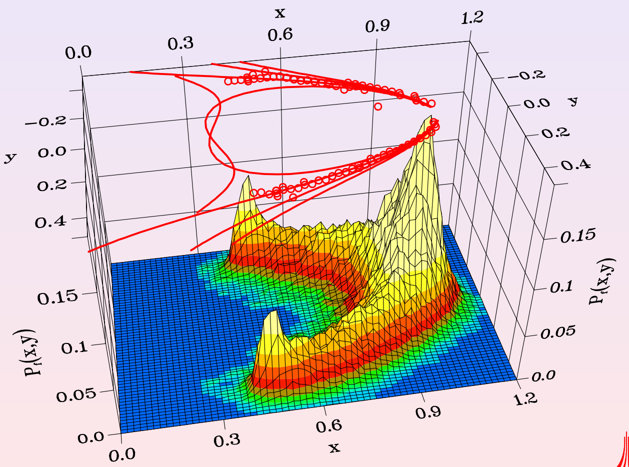

Maier & Stein optimal paths

- Again, two experiments.
- Showing both outgoing fluctuational paths (red) and returning relaxational paths (blue).
- Lines are Maier & Stein theory, points are Lancaster experiment.
- Rotational flow of the probability density (predicted by Onsager).

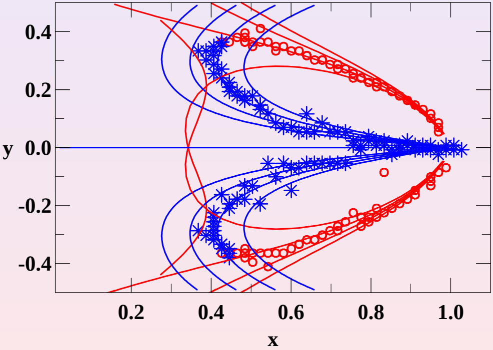

Fluctuational escape from a chaotic attractor

- Escape from point attractors and limit cycles has been intensively studied over many years.
- But how does fluctuational escape take place from a chaotic attractor?
- No theory exists – but experiments are entirely feasible.
- Have used both digital and analogue simulation.
- So far, we have studied –
  - Tilted Duffing oscillator.
  - Lorenz attractor.
  - Class-B laser equations (control).
- Summarise results from the tilted Duffing...

Tilted Duffing oscillator (TDO)

Consider the periodically-driven, tilted, underdamped, Duffing oscillator,

$$\ddot{x} + 2\Gamma\dot{x} + \omega_0^2 x + \beta x^2 + \gamma x^3 = A\cos(\Omega t) + \xi(t),$$
$$\langle\xi(t)\rangle = 0, \quad \langle\xi(t)\xi(0)\rangle = 4kT\Gamma\delta(t),$$
$$\Gamma \ll \omega_f, \quad \frac{9}{10} < \frac{\beta^2}{\gamma\omega_0^2} < 4.$$

For the chosen parameter range –

- Chaos appears at relatively small driving amplitude, $A \simeq 0.1$.
- A quasi-attractor then coexists with a stable limit cycle.
- We examine fluctuational escape from the quasi-attractor.

Basins of attraction

- Basins of stable limit cycle SC1 (shaded) and chaotic attractor (white).
- The unstable saddle cycle of period 1 (UC1) marks the boundary between the basins.
- Saddle cycle of period 3 is marked with $+$s.

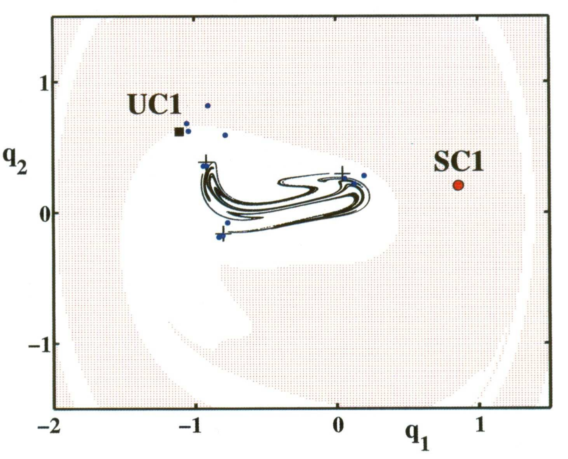

Existence of an optimal escape path

- Analogue simulation, showing a bunch of escape paths.
- They are nearly coincident, implying existence of an optimal path for escape.
- Red triangles show calculated saddle cycle of period 1.

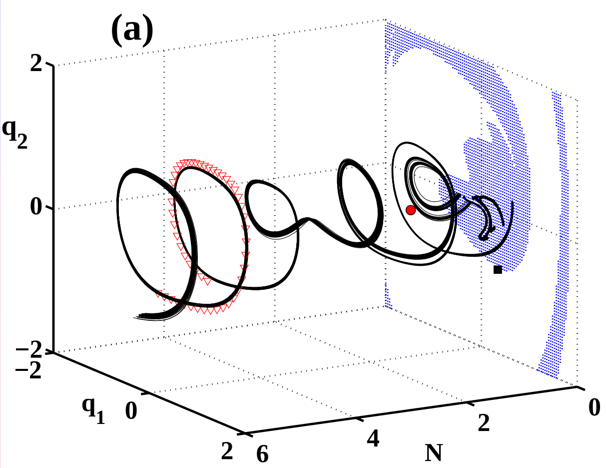

Escape goes via saddle cycles

- Escape evidently goes via saddle cycles UC5 (green) UC3 (black) and UC1 (red).
- Driven by optimal force (inset).
- Once on UC1, no more force is required to reach stable cycle SC1 (blue).

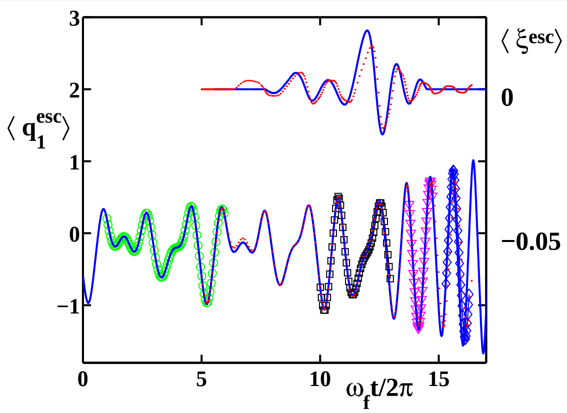

Control of noise-free system??

- Does the experimentally-determined optimal force (1) cause escape in the noise-free system?
- Yes! (1) is applied at increasing amplitude until escape occurs.
- Approximations to (1) also cause escape, but cost extra energy –
    - Approximated with sine-waves (2).
    - And with rectangular pulses (3).
    - Optimal force distorted by an arbitrary perturbation (4).
    - Standard open-plus-closed-loop (OPCL) control (5).
- The measured optimal force really does seem to be energy-optimal.

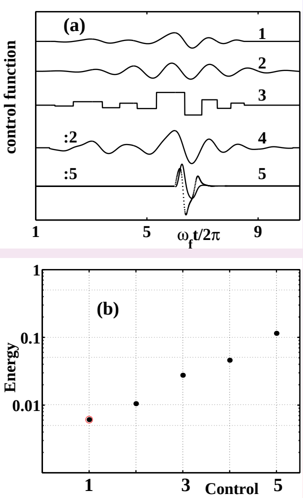

Laser – single-mode rate equations

We consider the single-mode rate equations -

$$\begin{cases} \frac{du}{dt} & = vu(y-1), \\ \frac{dy}{dt} & = q + k\cos(\omega t) - y - yu + f(t), \end{cases}$$

where –

- $u \propto$ density of radiation
- $y \propto$ carrier inversion
- v is ratio of photon damping and carrier inversion rates
- Cavity loss is normalised to unity
- Pumping rate has constant term $q +$ periodic component
- $f(t)$ is an additive unconstrained control function

Map

- For class-B lasers, $v \sim 10^3 - 10^4$; get spiking regimes for deep modulation of pumping rate.
- Obtain solutions from corresponding 2-D Poincaré map –

$$\begin{cases} c_{i+1} = & q + G(c_i, \psi_i)e^{-T} + K\cos(\omega T + \psi_i) + f_i, \\ \varphi_{i+1} = & \varphi_i + \omega T, \mathrm{mod}\ 2\pi, \end{cases}$$

- $G(c_i, \psi_i) = c_i - g - q - K\cos\psi_i$, $K = k(1 + \omega^2)^{-1/2}$, and $\psi_i = \varphi_i - \arctan(\omega)$.
- Control function f_i is now defined in discrete time.
- $g = g(c_i)$ is positive root of

$$g - c_i(1 - \exp(-g)) = 0$$

Map and its range of validity

- $T = T(c_i, \varphi_i)$ is positive root of

  $$(q-1)T+G(c_i,\psi_i)(1-e^{-T})+K\omega^{-1}[\sin(\omega T+\psi_i)-\sin\psi_i] = 0.$$
- c_i, φ_i correspond to the inversion of population $y(t_i)$ and to the phase of modulation $\varphi_i = \omega t_i$, mod 2π at the moments t_i of pulse onset when $u(t_i) = 1, \dot{u}(t_i) > 0$.
- $g(c_i)$ denotes the energy of the pulse.
- $T(c_i, \varphi_i)$ gives the time interval between sequential pulses.
- Map was derived by asymptotic integration to accuracy $O(v^{-1})$, so it is valid for –
  - $q, k, \omega \ll v$
  - $c_i > 1 + O(v^{-1})$

Generalized multistability of map

- Fixed points of the map determine spiking solutions at multiples of the driving period, at $T_n = nT_M$, where $T_M = 2\pi/\omega$ is the driving period.
- They are born through a saddle node bifurcation at modulation threshold

$$k_{sn} = \sqrt{1+\omega^2}[q - C_n - g_n(e^{T_n} - 1)^{-1}].$$

- The stable cycles undergo period-doubling bifurcations beyond

$$k_{pd} = \frac{\sqrt{1+\omega^2}}{\omega}(q-1)\left[1 + 2\pi\left(\frac{qnT_n}{12}\right)^2 + O(T_n^4)\right].$$

- Hence we determine analytically regions of generalized multistability, numbers of coexisting cycles, and approximatel locations of the saddles and stable cycles.

Basin of attraction for flow system

- Study controlled migration from stable cycle C_3 to saddle cycle S_3.
- After reaching S_3, system no longer needs an applied force.
- Two kinds of force are considered –
  - Continuous
  - Impulses

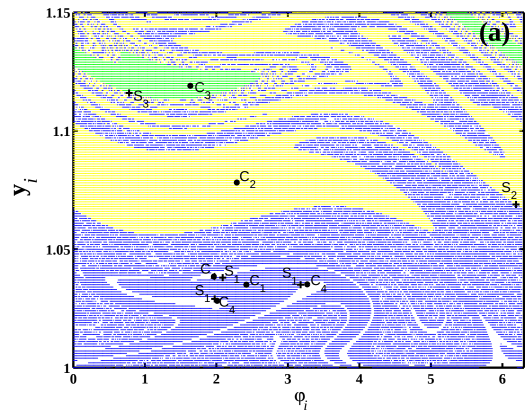

The control problem

- Consider the energy-optimal control problem –
  - How can system with unconstrained control function $f_c(t)$ or $f_d(t)$ be steered between coexisting states such that its "cost" functional

$$J_c = \inf_{f \in F} \frac{1}{2} \int_{t_0}^{t_1} f^2(t) dt, \quad \text{or} \quad J_d = \inf_{f \in F} \frac{1}{2} \sum_{i=1}^{N} f_i^2$$

    is minimized? Here t_1, N are unspecified and F is the set of control functions.
  - In general, a *very* challenging problem.
- Tackled it via ideas from optimal escape – correspondence of Wentzel-Freidlin Hamiltonian in fluctuation theory with Pontryagin's Hamiltonian in control theory.

Continuous control results

- Problem was solved by prehistory approach and numerical solution of boundary value problem.
- Variation of the coordinate $x(t)$ during migration from stable cycle C_3 to saddle cycle S_3.
- Variation of the control force $f(t)$ during the migration.
- In noise-free system, showed that direct application of the optimal force as a control force does cause $C_3 \rightarrow S_3$ migration.

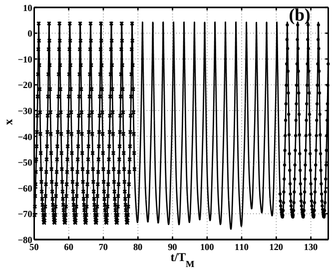

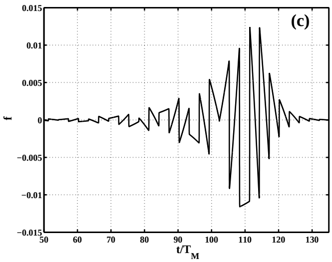

Summary

1. Large fluctuations do occur via optimal paths
2. Patterns of optimal paths and some singularities (not caustics) are physical observables.
3. For electronic models, the optimal force can be measured.
4. In equilibrium, fluctuations display time-reversal symmetry (if the p-dimension is ignored).
5. Fluctuations in nonequilibrium systems are irreversible.
6. Escape from chaotic attractors also occurs via optimal paths.
7. Intimate connection between the optimal fluctuational force and the energy-optimal control force in the noise-free system.

Acknowledgements and references

Acknowledgements

Many collaborators, including especially
Mark Dykman (Michigan State), Elena Grigorieva (Minsk), Natalia Khovanova (Lancaster), Riccardo Mannella (Pisa), and Nigel Stocks (Warwick).

The work has been supported mainly by EPSRC.

Selected references

1. M I Dykman, P V E McClintock, V N Smelyanski, N D Stein and N G Stocks, “Optimal paths and the prehistory problem for large fluctuations in noise-driven systems"; *Phys. Rev. Lett.* **68**, 2718-2721 (1992).
2. D G Luchinsky and P V E McClintock, “Irreversibility of classical fluctuations studied in electrical circuits”; *Nature* **389**, 463–466 (1997).
3. I A Khovanov, D G Luchinsky, R. Mannella and P V E McClintock, “Fluctuations and the energy-optimal control of chaos”, *Phys. Rev. Lett.* **85**, 2100–2103 (2000).
4. D G Luchinsky, “Deterministic patterns of noise and the control of chaos”, *Contemporary Phys.* **43**, 379–395 (2002).
5. D G Luchinsky, S Beri, R Mannella, P V E McClintock, and I A Khovanov, “Optimal fluctuations and the control of chaos”, *Int. J. of Bifurcation and Chaos* **12**, 583–604 (2002).
6. I A Khovanov, N A Khovanova, E V Grigorieva, D G Luchinsky, P V E McClintock, “Dynamical control: comparison of map and continuous flow approaches”, *Phys. Rev. Lett.* **96**, 083903 (2006).